Food Innovation and Advances

ARTICLE

Open Access

https://doi.org/10.48130/fia-0026-0005

Food Innovation and Advances **2026**, 5(1): 76–86

Unraveling the physicochemical, structural, and anti-allergic properties of *Laminaria japonica* fucoidan: a structure-function perspective

Xiao Wu[1], Wenjuan Wang[1], Yuxin She[1], Jingwen Yang[1], Xueni Huang[1], Zihao Li[1], Zhenxing Li[1], Hong Lin[1], Hang Xiao[2] and Ziye Zhang[1*]

[1] *State Key Laboratory of Marine Food Processing & Safety Control, College of Food Science and Engineering, Ocean University of China, Qingdao 266404, China*
[2] *Department of Food Science, University of Massachusetts, Amherst, MA 01003, USA*
* Correspondence: zhangziye@ouc.edu.cn (Zhang Z)

Abstract

Laminaria japonica fucoidan (LJF) is a composite macromolecule with anti-allergic ability. This study investigated the effects of NaCl elution on the physicochemical, structural properties, and anti-allergic ability of LJF, to provide a theoretical basis for the in-depth insights into LJF. The LJF eluted fractions (LJF-1 and LJF-2) using different NaCl concentrations were primarily composed of carbohydrates that are rich in fucose, sulfate radical, uronic acid, and rhamnose, monosaccharide compositions and Fourier transform infrared spectroscopy confirmed the presence of multiple functional components (e.g., sulfate radical and β-glycosidic bonds) in LJF-1 and LJF-2 varied significantly under elution with different NaCl concentrations. As to the hyaluronidase inhibition rate, LJF-2 performed the most potent hyaluronidase inhibition ability, which was particularly attributed to its high sulfate radical and rhamnose contents, LJF-2 was selected for further anti-allergic ability investigation. As for the anti-allergic ability, LJF-2 could mostly decline NO and ROS levels in RAW 264.7 macrophages, and inhibited the release of pro-inflammatory mediators from lipopolysaccharides (LPS)-stimulated macrophages, and inhibited the release of β-hexosaminidase, histamine, Ca^{2+}, and ROS from RBL-2H3 mast cells, reduced the degranulation degree and histamine release by down-regulating STIM1 and PRTC genes that are associated with the calcium influx signaling pathway. Therefore, LJF-2 performed the strongest anti-allergic ability, which depended on the physicochemical and structural properties that were significantly influenced by elution using different NaCl concentrations.

Citation: Wu X, Wang W, She Y, Yang J, Huang X, et al. 2026. Unraveling the physicochemical, structural, and anti-allergic properties of *Laminaria japonica* fucoidan: a structure-function perspective. *Food Innovation and Advances* 5(1): 76–86 https://doi.org/10.48130/fia-0026-0005

Introduction

Food allergies, affecting 3%–4% of the global population, pose a significant public health and industrial challenge with no definitive cure. Current mitigation strategies focus on either reducing allergenicity via food processing, or modulating immune responses using natural bioactive compounds. Given the limitations of processing techniques in fully eliminating allergenic potential, the utilization of natural anti-allergic ingredients, such as fucoidans[1], represents a promising preventive approach.

Fucoidans are composite macromolecular compounds formed by glycosidic bonds linking aldoses or ketoses. As critical biological macromolecules, they could play pivotal functions in sustaining human physiological functions through the modulation of immune responses[1]. In recent years, algal fucoidans have garnered significant attention owing to their diverse biological activities (e.g., anti-allergy), and high safety, making them increasingly popular functional compounds.

Laminaria japonica is a rich algal source of fucoidans, and has extensive applications in food, dietary supplements, and functional compounds. In particular, fucoidan obtained from brown algae is an active substance that exhibits various biological activity functions[2], particularly *Laminaria japonica* fucoidan (LJF), which is an algal-derived fucoidan with minimal side effects, and diverse physiological activities, making it a key active ingredient for maintaining human health, and preventing various diseases[3]. To date, numerous functional activities of *Laminaria japonica* fucoidan have been confirmed through *in vitro* and *in vivo* investigations, including anti-allergy[3,4]. This work further investigated the physicochemical and structural features of fucoidans extracted from *Laminaria japonica*, and the stricture and anti-allergy ability relationship.

Unlike previous studies, which often focused on crude fucoidan extracts, this work systematically investigates how NaCl gradient elution modulated the physicochemical structure of *Laminaria japonica* fucoidan fractions, and directly linked these structural variations (particularly sulfate/uronic acid content and monosaccharide profile) to their anti-allergic efficacy at the molecular and cellular level. This structure-function approach provides novel mechanistic insights into the role of specific polysaccharide features in hyaluronidase inhibition, mast cell stabilization, and macrophage immunomodulation, which could provide a robust preclinical foundation for the application of LJF in food allergy prevention and treatment.

Materials and methods

Materials

Laminaria japonica was collected from Xiapu, Fujian Province, China; PBS buffer, citric acid buffer, and Triton X-100 were obtained from Solarbio Technology Co., Ltd. (Beijing, China); C48/80 and lipopolysaccharide (LPS) were purchased from Sigma-Aldrich (St. Louis, MO, USA); DEME culture medium and MEM culture medium were purchased from Shanghai Yuanpei Biotechnology Co. Ltd. (Shanghai, China); Fetal bovine serum (FBS). and EDTA-pancreatic enzyme were acquired from Thermo Scientific Inc. (Waltham, MA,

USA); β-Hexosaminidase was obtained from Shanghai Yuanye Bio-Technology Co., Ltd. (Shanghai, China); 2',7'-dichlorofluorescin (H2DCFDA) was obtained from GlpBio (Montclair, CA, USA); Fluo-4 AM and nitric oxide detection kits were obtained from Shanghai Biyuntian Biotechnology Co., Ltd. (Shanghai, China); Aluminum hydroxide adjuvant was obtained from Beijing Biosynthesis biotechnology Co., Ltd. (Beijing, China); Interleukin-1β (IL-1β), Interleukin-6 (IL-6), histamine, and TNF-α ELISA kits were obtained from Boster Biological Technology Co., Ltd. (Wuhan, China). Stromal Interaction Molecule 1 (STIM1), and Transient Receptor Potential Cation Channel Subfamily C Member 1 (TRPC1) were obtained from Sangon Biotech (Shanghai) Co., Ltd. All chemical reagents were analytical grade or better.

Extraction and purification of *Laminaria japonica* fucoidan (LJF)

Crude fucoidan was sequentially extracted from ground *Laminaria japonica* after lipid removal via Soxhlet extraction. Hot water extraction (80 °C, 1:30 w/v) was followed by ethanol precipitation, Sevage reagent deproteinization, dialysis (3.5 kDa), and lyophilization. The obtained crude fucoidan was purified via DEAE-52 cellulose column chromatography, employing gradient elution with 0.5 and 1.0 mol/L NaCl. The resulting fucoidan (LJF), 0.5 mol/L NaCl elute-fraction (LJF-1), and 1.0 mol/L NaCl elute-fraction (LJF-2) were collected, concentrated, dialyzed, and freeze-dried for subsequent characterization and bioactivity assessment.

Physicochemical properties analysis of LJF

Carbohydrate content analysis

Total carbohydrate content (with L-fucose as the standard) was quantified using the phenol-sulfuric acid method according to Bisso et al.[5], with slight modifications. Standard L-fucose solutions were prepared in deionized water at 20–200 μg/mL. Five milligrams of *Laminaria japonica* fucoidan were dissolved in 1 mL of distilled water, and 2.5 mL of concentrated sulfuric acid was carefully added. Samples were kept at 4 °C during preparation for stability. Then, 0.5 mL of 5% phenol solution was added to each sample, followed by incubation for 10 min with stirring, and 30 min in a 25 °C water bath. Absorbance was measured at 480 nm using a UV-Vis spectrophotometer (UV-2550, Shimadzu, Kyoto, Japan).

Sulphate radical content determination

The gelatin-barium chloride method was used to determine sulphate group content in LJF (with potassium sulphate as the standard), according to Álvarez-Viñas et al.[6], with minor modifications. A 500 mg sample of each fraction (LJF, LJF-1, LJF-2) was mixed with 3 mL of 1 mol/L HCl, and hydrolyzed in a boiling water bath for 4 h. After cooling to 25 °C, the solution was filtered. Then, 1 mL of filtrate was combined with 0.1 mL of 6 mol/L HCl, and 0.5 mL of 70% sorbitol under stirring. Afterwards, 1.0 g of $BaCl_2$ crystals was added, and absorbance was measured at 470 nm using a UV-Vis spectrophotometer (UV-2550, Shimadzu, Kyoto, Japan). Potassium sulphate was the reference.

Uronic acid content

Uronic acid content was quantified using the carbazole-sulfuric acid method, with D-glucuronic acid as the standard, following the procedures according to Roy et al.[7]. Firstly, standard solutions of D-glucuronic acid were prepared in deionized water at concentrations ranging from 50 to 250 μg/mL. A 1.0 mL aliquot of the diluted sample solution was mixed with 6 mL of concentrated sulfuric acid, vortexed thoroughly, and heated at 95 °C for 20 min. Following cooling to room temperature, 200 μL of a 0.15% carbazole ethanol solution was added, and the mixture was incubated at room temperature for 2 h. The absorbance was subsequently measured at 530 nm using a UV-Vis spectrophotometer (UV-2550, Shimadzu, Kyoto, Japan).

Protein content analysis

Protein content was quantified using the Kaomas Brilliant Blue method[8], with bovine serum albumin (BSA) as the standard. Standard solutions of BSA, ranging from 40 to 200 μg/mL, were prepared in deionized water. A 1.0 mL aliquot of the diluted BSA solution was mixed with 5.0 mL of Cauloblue G-250 staining solution, vortexed thoroughly, and incubated for 3–5 min at room temperature. The absorbance was subsequently measured at 595 nm using a UV-Vis spectrophotometer (UV-2550, Shimadzu, Kyoto, Japan), with the blank serving as the reference.

Structural characterization of LJF

Monosaccharide composition analysis

The monosaccharide composition of LJF was analyzed following a modified method based on Shi et al.[9]. Samples were hydrolyzed with 2 mol/L trifluoroacetic acid at 105 °C for 6 h. After evaporation and methanol washing, the hydrolysates were derivatized with PMP under alkaline conditions at 70 °C for 2 h. The derivatized mixtures were neutralized, extracted with trichloromethane, filtered, and analyzed by HPLC (Agilent 1260) equipped with a ZORBAX Eclipse Plus-C18 column. Elution was performed using a phosphate buffer/acetonitrile gradient (83:17, v/v) at 1 mL/min and 30 °C, with identification based on eight monosaccharide standards.

Fourier transform infrared spectroscopy (FT-IR) analysis

The fucoidan samples were analyzed using infrared spectral scanning using the potassium bromide compression method[10]. The FT-IR spectra of LJF, LJF-1, and LJF-2 were recorded using a Fourier transform infrared spectrometer (Nicolet iS10, Thermo Scientific, Madison, WI, USA). This was done by mixing 1.0 mg of LJF with 100 mg of potassium bromide powder, and grinding the mixture thoroughly. It was then pressed into a uniform and transparent sheet using a tablet press. This was followed by infrared scanning in the range of 4,000–500 cm^{-1}, and potassium bromide was used as a blank control to correct the background.

Particle size and zeta potential determination

LJF, LJF-1, and LJF-2 was completely dissolved in ultrapure water, and the concentration was set to 0.5 mg/mL. After dissolution, fucoidan particle size and zeta potential were measured using a nanoparticle size analyzer (Zetasizer Nano ZS90, Malvern Instruments Ltd., Malvern, UK)[11].

Hyaluronidase inhibition assay of LJF

Hyaluronidase inhibition rate of LJF

Hyaluronidase activity of LJF, LJF-1, and LJF-2 was determined by adapting the Morgan-Elso method with appropriate modifications[12]. The procedure involved mixing 700 μL of acetic acid-sodium acetate buffer, 100 μL of fucoidan solution, and 100 μL of hyaluronidase solution homogeneously, followed by incubation for 10 min at 37 °C in a water bath. Subsequently, 100 μL of sodium hyaluronate solution was added, mixed thoroughly, and incubated for an additional 15 min at 37 °C. The reaction was immediately terminated by adding cetyltrimethylammonium bromide (CTAB). After incubating the

mixture at room temperature for 10 min, the absorbance was measured at 400 nm using a UV-Vis spectrophotometer (UV-2550, Shimadzu, Kyoto, Japan). The inhibition rate was calculated using the following formula.

$$\text{Hyaluronidase inhibition rate (\%)} = \frac{(A-B)-(C-D)}{A-B} \times 100$$

where, A: $OD_{400\ nm}$ of buffer instead of fucoidan sample; B: $OD_{400\ nm}$ of fucoidan sample; C: $OD_{400\ nm}$ of buffer instead of enzyme solution; D: $OD_{400\ nm}$ of buffer instead of enzyme solution and fucoidan sample.

Fluorescence spectroscopic analysis of hyaluronidase inhibitory activity

The hyaluronidase solution (1.0 mg/mL), and fucoidan samples at varying concentrations were prepared in PBS. The hyaluronidase solution was mixed with fucoidan solutions in equal volumes, thoroughly vortexed, and incubated at 37 °C for 15 min. After centrifugation (10,000 r/min, 5 min), the supernatant was subjected to fluorescence spectral analysis. Fluorescence spectra were recorded under the following conditions: excitation wavelength at 280 nm, emission wavelength range of 300–400 nm, scan speed of 240 nm/min, and slit width of 5.0 nm.

RAW264.7 macrophage assay

Cell viability assessment

RAW264.7 cells were maintained in a culture medium consisting of 10% (v/v) fetal bovine serum (FBS), 90% MEM medium, and 1% triple antibiotic solution (penicillin-chloramphenicol-amphotericin). Cells were cultured in a cell incubator (Shanghai Heal Force Biomedical Technology Co. Ltd., Shanghai, China) at 37 °C and 5% CO_2[13]. Cell viability was evaluated with the Cell Counting Kit-8 (CCK-8) (C0037, Beyotime Biotechnology Co., Shanghai, China). RAW264.7 cells (1×10^4 cells/well) were seeded in 96-well plates, and incubated at 37 °C with 5% CO_2 for 24 h. The medium was then removed, and cells were washed three times with sterile PBS. LJF solutions (25, 50, 100, 200, 400 μg/mL) were added, and plates were incubated for 20 h. Afterwards, 10 μL of CCK-8 reagent was added per well, and incubated for 4 h. Absorbance at 450 nm was measured using a microplate reader (BioTek Synergy LX, Agilent, Santa Clara, CA, USA). The PBS-treated cells served as the control, and cell viability percentages were calculated.

Nitric oxide (NO) analysis

RAW 264.7 cells (5×10^4 cells/well) were seeded in 96-well plates, and incubated at 37 °C with 5% CO_2 for 24 h. The medium was aspirated, and cells were washed three times with PBS. Then, 1 μg/mL LPS was added to the positive control group, 1 μg/mL LPS with LJF samples (25, 50, 100 μg/mL) to the fucoidan treated group, and PBS to the negative control group. Cells were incubated for 24 h. Supernatants were collected, and NO levels were measured using the Griess kit (S0021, Biyuntian, Jiangsu, China).

Reactive oxygen species (ROS) analysis

RAW 264.7 cells (5×10^4 cells/well) were seeded in sterile black 96-well plates, and incubated for 24 h at 37 °C with 5% CO_2. The medium was aspirated, and cells were washed three times with PBS. Then, 1 μg/mL LPS was added to the positive control group, 1 μg/mL LPS with LJF samples (25, 50, 100 μg/mL) to the fucoidan-treated group, and DEME medium to the negative control group. Cells were incubated for 24 h. Afterward, cells were incubated with DCFH-DA probe for 30 min, washed three times with PBS, lyzed with 0.1% Triton X-100 in PBS, and fluorescence intensity was measured at the excitation wavelength of 488 nm, and the emission wavelength of 525 nm using a microplate reader (BioTek Synergy LX, Agilent, Santa Clara, CA, USA).

Gene expression of pro-inflammatory mediators

RAW264.7 cells (2 mL/well) were pipetted into 6-well plates (1×10^6 cells per well), then incubated at 37 °C in 5% CO_2 for 24 h, and treated with LPS (1 μg/mL) for 12 h. After the end of the culture, the old culture solution was sucked away, and the cells were fully moistened with sterile PBS buffer, and the cell precipitate was collected by a sterile enzyme-free cell scraper for immediate extraction of total RNA. The total RNA of RAW264.7 cells was isolated using the RNA-easy Isolation Reagent (R701-01, Vazyme, China). cDNA was synthesized from 1 μg of RNA using the ToloScript All-in-one RT EasyMix for qPCR (22107, Tolobio, Shanghai, China). The fold change in gene expression was calculated using the $2^{-\Delta\Delta CT}$ method with GAPDH as the reference. qRT-PCR cycling conditions: 95 °C for 30 s, followed by 40 cycles of 95 °C for 30 s, and 60 °C for 30 s. Real-time quantitative PCR (q-PCR) was performed with the following primers: GAPDH (5′-CGACCCCTTCATTGACCTCAA-3′, 5′-ATGCAGGGATGATGTTCTGGG-3′), IL-6 (5′-ACAAAGCCAGAGTCCTTCAGAG-3′, 5′-TTAGCCACTCCTTCT GTGACTC-3′), IL-1β (5′-AGATGAAGG GCTGCTTCCAAA-3′, 5′-GGGTATTGCTTGGGATCCACA-3′), TNF-α (5′-TCAGCCTCTTCTCATTCCTGC-3′, 5′-CTGGAAGACTCCTCCCAGGTA-3′).

RBL-2H3 mast cell assay

Cell viability assessment

RBL-2H3 cells were maintained in a culture medium consisting of 10% (v/v) fetal bovine serum (FBS), 90% MEM basal medium, and 1% triple antibiotic solution (penicillin-chloramphenicol-amphotericin). Cells were cultured in a Heal Force 90 cell incubator (Shanghai Heal Force Biomedical Technology Co., Ltd.) at 37 °C, and 5% CO_2[13]. The cell viability was evaluated using Cell Counting Kit-8 (CCK-8) (C0037, Beyotime Biotechnology Co., Shanghai, China). RBL-2H3 cells (1×10^5 cells/well) were seeded in 96-well plates and incubated at 37 °C with 5% CO_2 for 24 h. The medium was then removed, and cells were washed three times with sterile PBS. LJF samples (25, 50, 100, 200, 400 μg/mL) were added, and plates were incubated for 20 h. Afterwards, 10 μL of CCK-8 reagent was added per well and incubated for 4 h. Absorbance at 450 nm was measured using a Enzyme-linked immunosorbent assay reader (CMax Plus, Molecular Devices, USA). Untreated cells served as the control, and cell viability (%) was calculated[14].

Effects of LJF on the degranulation of RBL-2H3 mast cells

RBL-2H3 cells (1×10^5 cells/well) were cultured in an incubator with a concentration of Anti-DNP-IgE (5% CO_2 at 37 °C) overnight. After that, MEM containing fucoidan (25, 50, 100 μg/mL, 100 μL/well) was pipetted to incubate at 37 °C for 2 h. After washing, DNP-BSA (100 μL/well) was pipetted for incubation for 1 h. Afterwards, cells are lysed with 1.0% Triton X-100 solution, with lysates collected. Then, 50 μL/well of cell supernatant was transferred into 96-well plate and incubated with 50 μL/well of 0.1 mol/L citrate buffer (pH = 4.5) containing 1.2 mmol/L 4-Nitrophenyl N-acetyl-β-d-glucosaminide for 90 min. Afterwards, 100 μL/well of sodium carbonate buffer (0.4 mol/L Na_2CO_3) was pipetted to stop the reaction. The $OD_{405\ nm}$ was recorded using an Enzyme-linked immunosorbent assay reader (CMax Plus, Molecular Devices, CA, USA), and the β-hexosaminidase activity (%) was calculated to reflect the degranulation degree[15].

Histamine content was measured using the fluorescent histamine method[16]. Briefly, 1,000 μL of supernatant was mixed with 200 μL of 1 mol/L NaOH and 50 μL of o-benzoyldialdehyde solution (1%)

in a light-protected tube, reacted for 4 min in the dark, and terminated with 100 μL of 3 mol/L HCl. After centrifugation (10,000 r/min, 15 min), 200 μL of supernatant was transferred to a black 96-well plate, and fluorescence was measured (excitation: 360 nm, emission: 450 nm) using a Multifunctional microplate reader (BioTek Synergy LX, Agilent, Santa Clara, CA, USA). Histamine content was quantified using a standard curve.

Reactive oxygen species (ROS) analysis

RBL-2H3 cells (1×10^5 cells/well) were cultured in an incubator with a concentration of Anti-DNP-IgE (5% CO_2 at 37 °C) overnight. Afterwards, LJF samples (25, 50, 100 μg/mL) solutions were used for a certain period of time, and DCFH-DA was used for 30 min. After that, 1.0 μg/mL of DNP-BSA was used for 1 h excitation and treatment with 1.0% Triton X-100 solution. The excitation wavelength of 488 nm and the emission wavelength of 525 nm were used to quantitatively detect the level of ROS secretion by a multifunctional microplate reader (BioTek Synergy LX, Agilent, Santa Clara, CA, USA).

Calcium ion (Ca^{2+}) analysis

RBL-2H3 cells (1×10^5 cells/well) were cultured in an incubator with a concentration of Anti-DNP-IgE (5% CO_2 at 37 °C) overnight. After that, LJF samples (25, 50, 100 μg/mL) were sequentially treated for a certain period of time, and Fluo-4 AM was used for 30 min. After that, 1.0 μg/mL of DNP-BSA was used for 1 h of excitation and treatment with 1.0% Triton X-100 solution. The excitation wavelength of 488 nm and the emission wavelength of 520 nm were used to quantitatively detect the level of Ca^{2+} secretion by a multifunctional microplate reader (BioTek Synergy LX, Agilent, Santa Clara, CA, USA).

Cytokine secretion determination

The total RNA of RBL-2H3 cells was isolated using the RNA-easy Isolation Reagent (R701-01, Vazyme, China). cDNA was synthesized from 1 μg of RNA using the ToloScript All-in-one RT EasyMix for qPCR (22107, Tolobio, Shanghai, China). The fold change was calculated using the $2^{-\Delta\Delta CT}$ method with β-actin as the reference. q-PCR cycling conditions: 95 °C for 30 s, followed by 40 cycles of 95 °C for 30 s and 60 °C for 30 s. Real-time quantitative PCR (q-PCR) was performed with the following primers: β-action (5′-TTGAACACGGC ATTGTCACC-3′, 5′-TTTTCACGGTTGGCCTTAGG-3′), STIM1 (5′-TTTTGCC GGGATTGACAAGCC-3′, 5′-ATCAGCTTGTGGATGTTGCG-3′), TRPC1 (5′-ATTGCGTAGATGTGCTTGGGG-3′, 5′-TGCCACCAAAAGTGCATCTG-3′).

Statistical analysis

All results are expressed as the mean ± standard deviation (SD) of three independently repeated experiments. $p < 0.05$ was considered statistically significant. Count data were analyzed for significant differences after square root transformation. In the graphs, different letters indicate significant differences between groups ($p < 0.05$), while the same letters indicate no significant differences ($p > 0.05$).

Results

Chemical composition of LJF

Fucoidan, a sulfated polysaccharide predominantly derived from seaweed, exhibited a broad spectrum of biofunctional properties, such as anti-allergy. Nevertheless, its bioactivity is highly dependent on structural characteristics such as molecular weight distribution, monosaccharide profile, conformational features, degree of sulfation, and sulfate group positioning[17]. Therefore, comprehensive characterization of the physicochemical attributes of *Laminaria japonica* fucoidan is crucial for elucidating its anti-allergic mechanisms. As presented in Table 1, the compositional analysis of *Laminaria japonica* fucoidan before and after purification revealed distinct physicochemical parameters. The neutral saccharide fraction accounted for 43.93% ± 0.08% of the purified sample, whereas uronic acid, quantified via the carbazole-sulfate assay, constituted 11.18% ± 0.17%. Sulfate groups, determined by gelatin-barium chloride titration, were present at 23.53% ± 0.67%, while residual protein contamination was minimal (1.18% ± 0.37%). The total carbohydrate content of LJF (43.93% ± 0.08%) confirmed the efficacy of the extraction protocol detailed in section "Extraction and purification of *Laminaria japonica* fucoidan (LJF)". Additionally, the low protein content demonstrated the successful protein removal during purification (section "Physicochemical properties analysis of LJF"), yielding a highly refined fucoidan preparation.

After NaCl elution, the 0.5 mol/L and 1.0 mol/L eluted fractions were designated as LJF-1 and LJF-2, respectively (Fig. 1). The compositional profiles of these fractions before and after elution were summarized in Table 1. NaCl elution resulted in a significant increase in sulfate radical content, promoting from 23.53% ± 0.67% (LJF) to 28.72% ± 0.58% (LJF-1), and 35.07% ± 0.23% (LJF-2), alongside elevated uronic acid levels promoted from 11.18% ± 0.17 % (LJF) to 14.26% ± 0.21% (LJF-1), and 17.20% ± 0.10% (LJF-2), respectively. Previous studies have established a strong association between fucoidan bioactivity and the abundance of uronic acid and sulfate radical[18]. Notably, the degree of sulfation (DS), reflecting the substitution of hydroxyl groups by sulfate esters, plays a pivotal role in modulating fucoidan's structural and functional properties[19]. Sulfate radicals are known to potentiate immune responses, and

Table 1. Physicochemical properties of LJF, LJF-1, and LJF-2 after NaCl elution.

LJF types	Carbohydrate content (%)	Uronic acid (%)	Sulfate radical (%)	Protein content (%)
LJF	43.93 ± 0.08	11.18 ± 0.17	23.53 ± 0.67	1.18 ± 0.37
LJF-1	54.91 ± 0.10	14.26 ± 0.21	28.42 ± 0.58	1.09 ± 0.22
LJF-2	62.29 ± 0.09	17.20 ± 0.10	35.07 ± 0.23	0.60 ± 0.17

LJF: *Laminaria japonica* fucoidan; LJF-1: *Laminaria japonica* fucoidan with 0.5 mol/L NaCl elution; LJF-2: *Laminaria japonica* fucoidan with 1.0 mol/L NaCl elution.

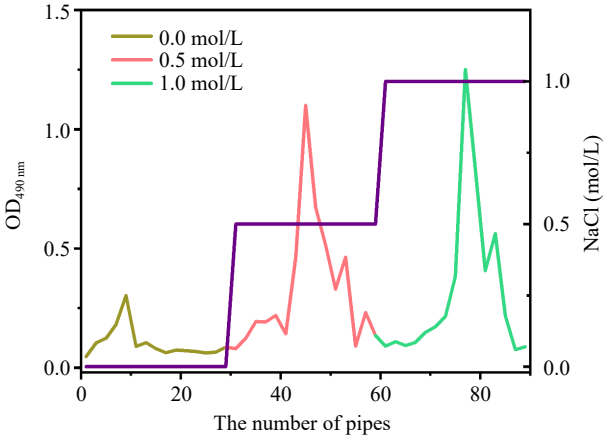

Fig. 1 The LJF elution curves with different NaCl concentrations. Note: LJF: *Laminaria japonica* fucoidan; LJF-1: *Laminaria japonica* fucoidan with 0.5 mol/L NaCl elution; LJF-2: *Laminaria japonica* fucoidan with 1.0 mol/L NaCl elution.

their synergistic interaction with acetyl groups has been proposed as an effective adjuvant framework for augmenting mucosal, cellular, and humoral immunity[20]. Additionally, localized sulfate clustering has been identified as a critical determinant for binding proteins[21]. Given the well-documented correlation between sulfate radical/uronic acid content and bioactivity, the enhanced compositional profiles of LJF-1 and LJF-2 suggested a potential superiority in biological efficacy compared to LJF.

Structural properties of LJF

Monosaccharide compositions

As a structurally heterogeneous sulfated polysaccharide predominantly composed of fucose residues, fucoidan served as a biologically active ion-modulating compound localized in algal cell walls[22]. This macromolecule typically exists in complex association with various neutral and acidic monosaccharides, forming intricate polysaccharide architectures. The anti-allergy efficacy of fucoidan has been demonstrated to be strongly dependent on its monosaccharide compositions. Particular monosaccharide motifs, including mannose, glucuronic acid, and fucose configurations, have been shown to exhibit molecular recognition properties toward pro-inflammatory factors, thereby potentiating their therapeutic effects[23]. This structure-activity relationship underscores the necessity for rigorous compositional characterization when investigating the anti-allergic ability of fucoidan.

The anti-allergic activity of fucoidans is structurally dependent, with key monosaccharides like mannose, glucuronic acid, and fucose contributing to bioactivity via specific molecular interactions[23]. Compositional analysis (Fig. 2a) revealed that *Laminaria japonica* fucoidan fractions (LJF, LJF-1, LJF-2) contain nine monosaccharides, with distinct profiles modulated by NaCl elution. LJF-2 showed a notable enrichment in rhamnose (21.42%), a bioactive 6-deoxyhexose linked to immunomodulation[24,25]. The variable distribution of fucose and mannose across fractions suggests complex structure-function relationships, highlighting the influence of isolation methods and source variability on fucoidan composition and anti-allergic efficacy.

Fourier transform infrared (FT-IR) spectroscopy

Fourier Transform Infrared Spectroscopy (FT-IR) was employed to characterize the structural features of *Laminaria japonica* fucoidans. The FT-IR spectral analysis (Fig. 2b) demonstrated consistent functional group profiles among LJF, LJF-1, and LJF-2, confirming that NaCl elution preserved the fundamental molecular groups of these polysaccharides. The FT-IR spectra exhibited characteristic vibrational modes at: 3,433 cm^{-1} (broad): The hydroxyl group stretching in carbohydrate moieties; 2,946 cm^{-1}: The ssymmetric methyl group vibrations; 1,643 cm^{-1}: The carbonyl stretching vibrations; 1421 cm^{-1}: The aliphatic C–H deformations; 1,250 cm^{-1}: The sulfate ester symmetric stretching (S=O); 1,061 cm^{-1}: The combined C–O–C ring stretching and C–O–H bending, indicative of pyranose configuration; 970 cm^{-1}: The β-configuration of interglycosidic linkages; 851 and 817 cm^{-1}: The C–O–S vibrations suggesting predominant C2 or C3 sulfation with minor C-4 substitution. These spectroscopic signatures collectively establish LJF as a β-linked pyranose polysaccharide with extensive sulfation, primarily at equatorial positions of the fucose residues. The invariant spectral patterns across different NaCl eluted fractions indicated that NaCl elutions maintained the essential structural integrity of the native fucoidan.

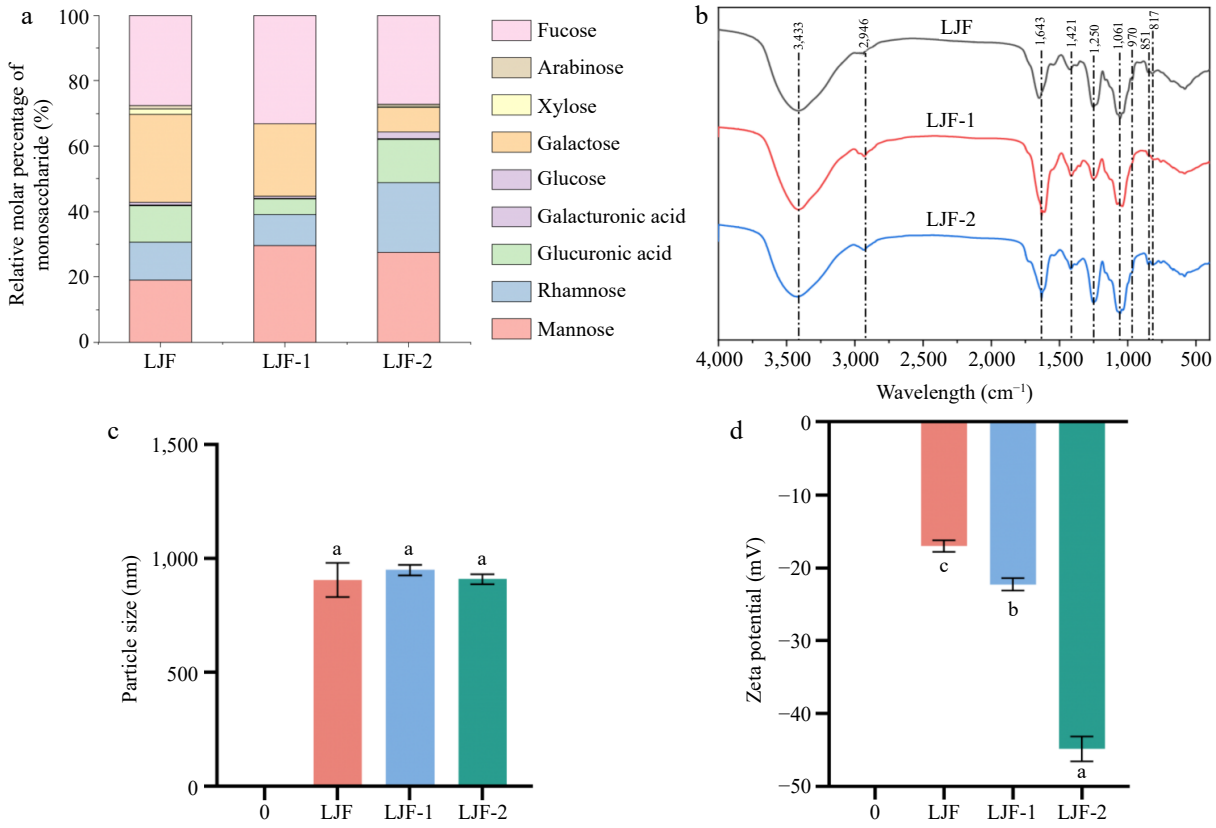

Fig. 2 The structural properties of LJF, LJF-1, and LJF-2. (a) Monosaccharide composition analysis. (b) Infrared spectral analysis. (c) Particle size analysis. (d) Zeta potential analysis. Note: LJF: *Laminaria japonica* fucoidan; LJF-1: *Laminaria japonica* fucoidan with 0.5 mol/L NaCl elution; LJF-2: *Laminaria japonica* fucoidan with 1.0 mol/L NaCl elution.

Particle size and zeta potential analysis

The hydrodynamic dimensions of fucoidan molecules served as an important indicator of molecular mass distribution and directly affect their biological absorption efficiency. Previous studies have established an inverse relationship between polysaccharide particle size and bioavailability[26]. Physicochemical characterization (Fig. 2c, d) revealed the following parameters for fucoidans: (1) Mean particle sizes: 906.67 ± 86.23 nm (LJF), 950.17 ± 17.63 nm (LJF-1), 910.2 ± 21.8 nm (LJF-2); (2) Surface charge potentials: −17.0 ± 0.82 mV (LJF), −22.27 ± 0.43 mV (LJF-1), −44.83 ± 0.83 mV (LJF-2). Notably, the zeta potential values showed fucoidan concentration-dependent attenuation during NaCl-gradient elution. This phenomenon may be resulted from the diminished intermolecular electrostatic forces and compromised interfacial stabilization, ultimately affecting colloidal stability[27]. The enhanced negative charge magnitude observed in LJF-2 (−44.83 mV) reflected superior dispersion stability, consistent with its elevated polysaccharide sulfation degree[28]. These findings collectively position LJF-2 as the most stable fraction among LJF, LJF-1, and LJF-2.

Hyaluronidase inhibition assay

Hyaluronidase inhibition rate

As a key mediator of mediating allergic reactions, hyaluronidase oversecretion could trigger allergic cascades, which making the hyaluronidase inhibition as a validated biomarker for assessing anti-allergic compounds[12]. As shown in Fig. 3a, the LJF dose dependent anti-allergy relationships demonstrated concentration-dependent hyaluronidase inhibition by different LJF fractions, revealing distinct anti-allergic ability. Notably, LJF exhibited paradoxical behavior that achieved the lowest hyaluronidase inhibition rate (1.6%) at 0.4 mg/mL, while the hyaluronidase inhibition rate significantly declined to 23.66% at a higher LJF concentration (1.0 mg/mL). This nonlinear response reflected the characteristic nonspecific binding tendencies of high-molecular-weight polysaccharides[29]. The crude LJF may contain interfering macromolecules that: (1) Form non-productive enzyme complexes; (2) Induce colloidal aggregation at higher concentration (e.g., 1.0 mg/mL) than 0.4 mg/mL; (3) Generate spectrophotometric artifacts through light scattering[30]. These experimental artifacts, consistent with observed inhibition trends, underscore the necessity of purified fractions for reliable bioactivity assessment. The concentration-dependent interference mechanisms explain why LJF demonstrated apparent loss of anti-allergic ability at elevated concentrations, invalidating its direct use in quantitative evaluations.

Compared with LJF, the LJF-1 performed a much stronger hyaluronidase inhibition rate than LJF, while the LJF-1 performed a lower hyaluronidase inhibition rate of LJF-1 at higher concentrations in a dose-dependent manner, while there is still a 83.6% hyaluronidase inhibition rate at 1.0 mol/L of LJF-1. This might be due to the fact that lower sulfated fucoidan demonstrated a proportional weaker hyaluronidase inhibition with higher concentration, though their peak efficacy falls short of highly sulfated analogs. Both sulfate density and spatial configuration collectively governed the fucoidan-hyaluronidase interaction stability. Structural deficiencies in low-sulfate variants hindered the complete occupancy of the enzymatically active sites of hyaluronidase[31].

Notably, compared with LJF and LJF-1, LJF-2 attained the lowest hyaluronidase inhibition rate (79.86%) at 0.4 mg/mL, then surpassed the hyaluronidase inhibition rate peak of LJF-1. Within the concentration of 0.2–0.4 mg/mL, LJF-2 exhibited decreased hyaluronidase inhibition rate. Beyond this threshold (0.4 mg/mL), LJF-2 performed the highest hyaluronidase inhibition rate, inducing more occupancy of the enzymatically active sites of hyaluronidase[32]. Moreover, the sulfate moieties were established as critical determinants of anti-allergic properties in algal fucoidans[33]. Higher sulfated fucoidans could greater suppress mast cell degranulation by 82% and curtail Th2 cytokine (IL-4, IL-13) release by 75%, whereas hyaluronidase inhibition contributes merely 22% to their overall efficacy[20].

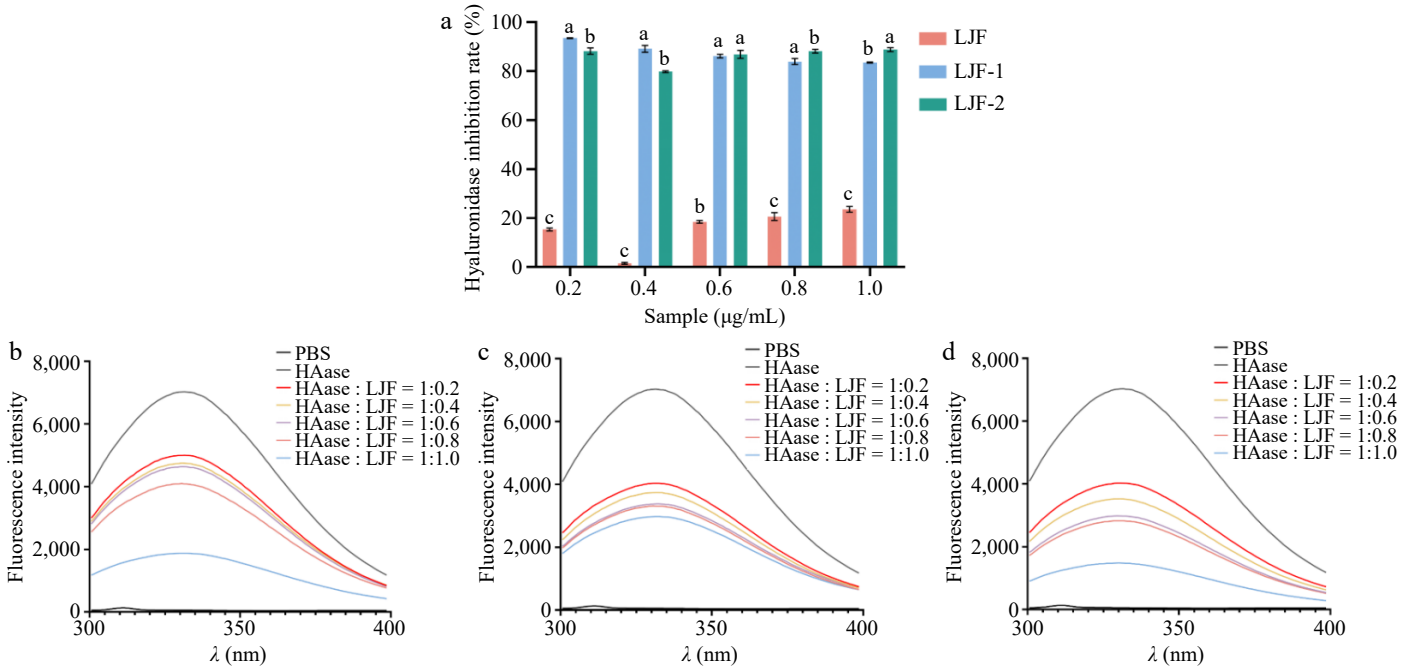

Fig. 3 Hyaluronidase inhibition assay of LJF, LJF-1, and LJF-2. (a) The hyaluronidase inhibition rate of LJF, LJF-1, and LJF-2. (b) Effects of LJF on the changes of hyaluronidase fluorescence intensity. (c) Effects of LJF-1 on the changes of hyaluronidase fluorescence intensity. (d) Effects of LJF-2 on the changes of hyaluronidase fluorescence intensity. Note: LJF: *Laminaria japonica* fucoidan; LJF-1: *Laminaria japonica* fucoidan with 0.5 mol/L NaCl elution; LJF-2: *Laminaria japonica* fucoidan with 1.0 mol/L NaCl elution.

This underscored the predominance of immunomodulatory mechanisms over direct enzymatic blockade. Given the physicochemical profiling and hyaluronidase inhibition rate of LJF, LJF-1, and LJF-2, LJF-2 emerged as the most potent hyaluronidase inhibitor, characterized by the highest sulfate content and superior *in vitro* anti-allergic performance (with the highest hyaluronidase inhibition rate). Therefore, LJF-2 were selected to investigate the anti-allergic ability of NaCl eluted fucoidans.

Fluorescence spectral analysis of hyaluronidase activity by LJF

As shown in Fig. 3b–d, the fluorescence analysis revealed that hyaluronidase exhibited a strong emission peak at 333 nm. As the increased concentrations of LJF, LJF-1, and LJF-2, the fluorescence intensity of hyaluronidase at 333 nm decreased significantly in a dose-dependent manner, while the emission peak position remained unchanged. This observation suggested that the interaction between the fucoidans (LJF, LJF-1, LJF-2) and hyaluronidase did not alter the microenvironment of tryptophan residues, supporting a non-covalent binding mechanism[34].

At a concentration of 1.0 mg/mL, LJF, LJF-1, and LJF-2 reduced the fluorescence intensity of hyaluronidase from 7,009.67 to 1,869, 2,968.33, and 1,468.67, respectively. Notably, LJF-2 demonstrated the highest inhibition efficiency (79.06%), surpassing LJF (73.34%), and LJF-1 (57.66%) by approximately 5.72% and 21.4%, respectively. Further analysis of the inhibition curves indicated that while both LJF and LJF-2 achieved comparable maximum inhibition at the highest concentration, LJF-2 exhibited more pronounced fluorescence quenching at medium and low concentrations. These results indicated that LJF-2 exhibited the enhanced binding affinity and superior inhibitory potency, demonstrating significant biological activity even at lower concentrations.

Combined with the results from physicochemical property determination (Table 1 and Fig. 2), hyaluronidase inhibition rate and fluorescence spectroscopy assays, LJF-2 emerged as the most effective inhibitor of hyaluronidase, exhibiting the highest sulfate content and superior *in vitro* anti-allergic activity (with the highest hyaluronidase inhibition rate and fluorescence spectroscopy inhibition). Therefore, LJF-2 were selected to further investigate the anti-allergic ability of NaCl eluted fucoidans in subsequent experiments.

RAW264.7 macrophage assay

Effect on RAW264.7 cell viability

The macrophages induced pro-inflammatory reactions are key mediators during allergic reactions. To investigate the anti-allergic activity of LJF-2, the RAW264.7 macrophage cells was firstly used to elucidate the effects of LJF-2 on the pro-inflammatory reactions during allergic reactions. Cellular toxicity was first assessed through CCK-8 proliferation assays to establish the non-cytotoxic concentration range. Experimental data presented in Fig. 4a demonstrated that LJF-2 treatment at doses between 25 and 400 μg/mL maintained cellular viability without statistically significant reduction ($p < 0.05$), confirming the biocompatibility of LJF-2 within this concentration range. Based on these safety profile results and considering reagent optimization, the concentration range of 25–100 μg/mL was selected for the subsequent experimental investigations.

Effects on RAW264.7 generation of NO and ROS

The lipopolysaccharide (LPS)-activated RAW 264.7 macrophages serve as an established cell model for studying the pro-inflammatory inhibition of LJF-2 during anti-allergic reactions, characterized by nitric oxide (NO) and proinflammatory cytokines through activation of multiple pro-inflammatory signaling cascades. The enzymatic conversion of L-arginine to NO, mediated by inducible nitric oxide synthase (iNOS), represented a key biochemical pathway involved in numerous physiological processes, including immune regulation, vascular homeostasis, and neural signaling[35]. Under inflammatory conditions induced by LPS, macrophage activation resulted in pathological overproduction of NO coupled with elevated intracellular reactive oxygen species, creating a pro-oxidative state that contributes to cellular dysfunction. As evidenced in Fig. 4b, LPS stimulation markedly elevated NO production to 16.48 μmol/L ($p < 0.05$ vs. untreated controls). This pro-inflammatory response was significantly attenuated by LJF-2 administration, with measured NO concentrations declining to 13.24, 12.87, and 10.74 μmol/L at 25, 50, and 100 μg/mL, respectively, representing inhibition efficiencies of 19.66%, 21.90%, and 34.83%, respectively ($p < 0.05$). The concentration-dependent suppression of NO generation clearly demonstrates LJF-2's potent anti-pro-inflammatory activity during allergic reactions.

As depicted in Fig. 4c, the quantitative analysis demonstrated a substantial increase in reactive oxygen species (ROS) generation, with stimulated cells exhibiting 171.83% fluorescence intensity compared to baseline controls (normalized to 100%, $p < 0.05$). The oxidative stress response was significantly mitigated by LJF-2 administration, showing dose-responsive reductions to 164.46%, 148.20%, and 134.69% at concentrations of 25, 50, and 100 μg/mL, respectively ($p < 0.05$). This graded suppression of oxidative activity clearly indicated LJF-2's concentration-dependent capacity to attenuate pro-inflammation-induced ROS formation during allergic reactions.

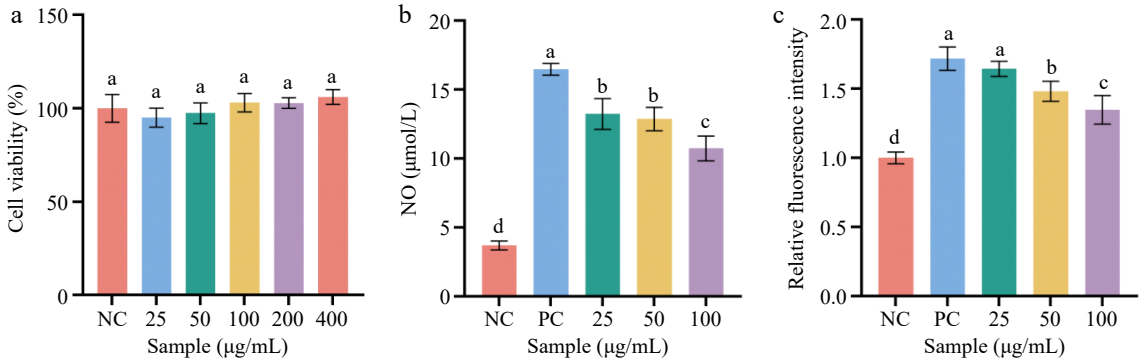

Fig. 4 Anti-proinflammatory effects of LJF-2. (a) Toxic effects of LJF-2 on RAW 264.7 macrophages. (b) Effects of LJF-2 on NO secretion. (c) Effects of LJF-2 on ROS secretion. Note: LJF-2: *Laminaria japonica* fucoidan with 1.0 mol/L NaCl elution; NC: Negative Control (untreated cells); PC: Positive Control (LPS-stimulated cells).

Effects on genes related to the pro-inflammatory pathway in RAW264.7 cells induced by LPS

The gene expression of pro-inflammatory mediators (e.g., TNF-α, IL-6, and IL-1β) (Fig. 5a–c) revealed the distinct transcriptional responses to inflammatory stimulation. As shown in Fig. 5a–c, the LPS-treated group served as the positive control (normalized to 1.0), and the unstimulated cells showed markedly reduced expression of proinflammatory markers ($p < 0.05$), confirming LPS's potent immunostimulatory effects in RAW 264.7 macrophages. Moreover, LJF-2 treatment produced a concentration-dependent suppression of key pro-inflammatory mediators: TNF-α expression declined to 1.03, 0.78, and 0.64; IL-6 expression decreased to 0.85, 0.81, and 0.55; and IL-1β expression reduced to 0.78, 0.77, and 0.68 at 25, 50, and 100 μg/mL doses of LJF-2, respectively (all $p < 0.05$ vs. LPS group). This graded transcriptional regulation, particularly through TLR4 pathway modulation, substantiates LJF-2's capacity to counteract LPS-induced pro-inflammation in a dose-responsive manner during allergic reactions.

RBL-2H3 mast cell assay

Effects on RBL-2H3 cell viability

After investigation of the pro-inflammation inhibition effects of LJF-2 during allergic reactions, the anti-allergic potential of *Laminaria japonica* fucoidans was further evaluated using RBL-2H3 mast cells. Firstly, the cytotoxicity assessments were performed via the CCK-8 assay to determine the impacts of LJF-2 on the cell viability. As illustrated in Fig. 6a, LJF-2 exhibited no significant reduction in RBL-2H3 proliferation at concentrations ranging from 25 to 400 μg/mL. Compared with the PBS control, the LJF-2 had no significant cytotoxicity on RBL-2H3 mast cells ($p > 0.05$), confirming the biocompatibility within this dosage range. To optimize reagent utilization, subsequent assays were conducted using LJF-2 at concentrations of 25–100 μg/mL.

Effects of RBL-2H3 on β-hexosaminidase and histamine levels

The mast cell degranulation response was evaluated using compound C48/80, a polymeric conjugate formed by the condensation of phenylethylamine with formaldehyde, which potently stimulates cytotoxic responses and promotes granular enzyme secretion. As reported by Zhang et al.[36], this compound induced substantial β-aminohexosaminidase release from RBL-2H3 cells. As presented in Fig. 6b, the RBL-2H3 cells had a marked elevation ($p < 0.05$) of β-aminohexosaminidase activity following C48/80 stimulation, with the PBS group exhibiting a β-aminohexosaminidase activity of 14.01%. Notably, LJF-2 administration at concentrations of 25, 50, and 100 μg/mL effectively suppressed this degranulation response, reducing β-aminohexosaminidase activity to 13.36%, 11.06%, and 10.79%, respectively ($p < 0.05$), demonstrating concentration-dependent inhibition of degranulation. Parallel measurements of histamine secretion revealed baseline levels of 12.22 ng/mL in the PBS group (Fig. 6c), which surged to 19.24 ng/mL upon C48/80 challenge ($p < 0.05$). This response was significantly attenuated by LJF-2 treatment, with histamine concentrations declining from 19.24 to 15.51, 13.92, and 10.13 ng/mL at LJF-2 concentrations of 25, 50, and 100 μg/mL ($p < 0.05$ vs. the model group). Collectively, these findings indicated that LJF-2 exerted dose-dependent suppression of both β-aminohexosaminidase activity and histamine release in RBL-2H3 mast cells.

Effects on the release of RBL-2H3 reactive oxygen species (ROS) and Ca^{2+}

Reactive oxygen species (ROS), comprising partially reduced oxygen metabolites, have been extensively implicated in the pathogenesis of hypersensitivity reactions, and inflammatory processes through oxidative stress mechanisms[37]. As shown in Fig. 6d, there was a substantial elevation (127.17%, $p < 0.05$) in ROS generation in stimulated positive cells, compared to PBS negative controls. This oxidative burst was effectively mitigated by LJF-2 administration, with fluorescence intensities declining to 118.82%, 117.60%, and 106.80% at concentrations of 25, 50, and 100 μg/mL, respectively ($p < 0.05$). As presented in Fig. 6e, the calcium ions, functioning as pivotal secondary messengers, critically regulate mast cell activation and subsequent mediator release through transmembrane flux modulation[37]. In the activated mast cells, a marked calcium influx was observed (fluorescence intensity: 33503, $p < 0.05$) that was concentration-dependently attenuated by LJF-2 treatment (30,363.67, 29,609.67, and 28,088 at 25, 50, and 100 μg/mL, respectively, $p < 0.05$). These findings collectively demonstrated LJF-2 could dose-dependently suppress both oxidative stress and calcium mobilization, substantiating its anti-allergic properties.

Effect of LJF on allergic cytokines in RBL-2H3 mast cells

Mast cell degranulation degree depended on the calcium concentration released from the endoplasmic reticulum (ER). Following ER calcium release, calcium channel-related proteins STIM1 and TRPC1 were activated[38], leading to the increased extracellular calcium influx and accelerated histamine release. Therefore, the expression

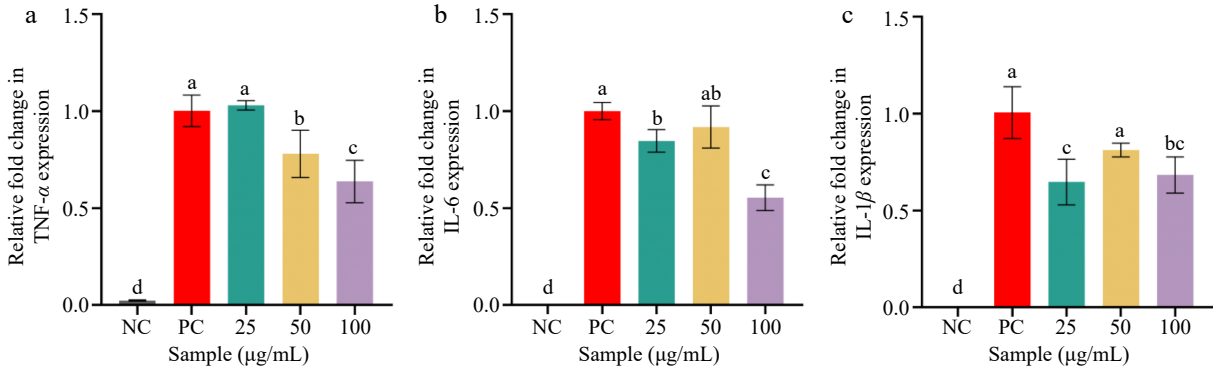

Fig. 5 Effects of LJF-2 on the gene expression level of pro-inflammatory mediators in RAW246.7 macrophages. (a) Effects of LJF-2 on TNF-α secretion. (b) Effects of LJF-2 on IL-6 secretion. (c) Effects of LJF-2 on IL-1β secretion. Note: LJF: *Laminaria japonica* fucoidan; LJF-1: *Laminaria japonica* fucoidan with 0.5 mol/L NaCl elution; LJF-2: *Laminaria japonica* fucoidan with 1.0 mol/L NaCl elution; NC: Negative Control (untreated cells); Positive Control (LPS-stimulated cells).

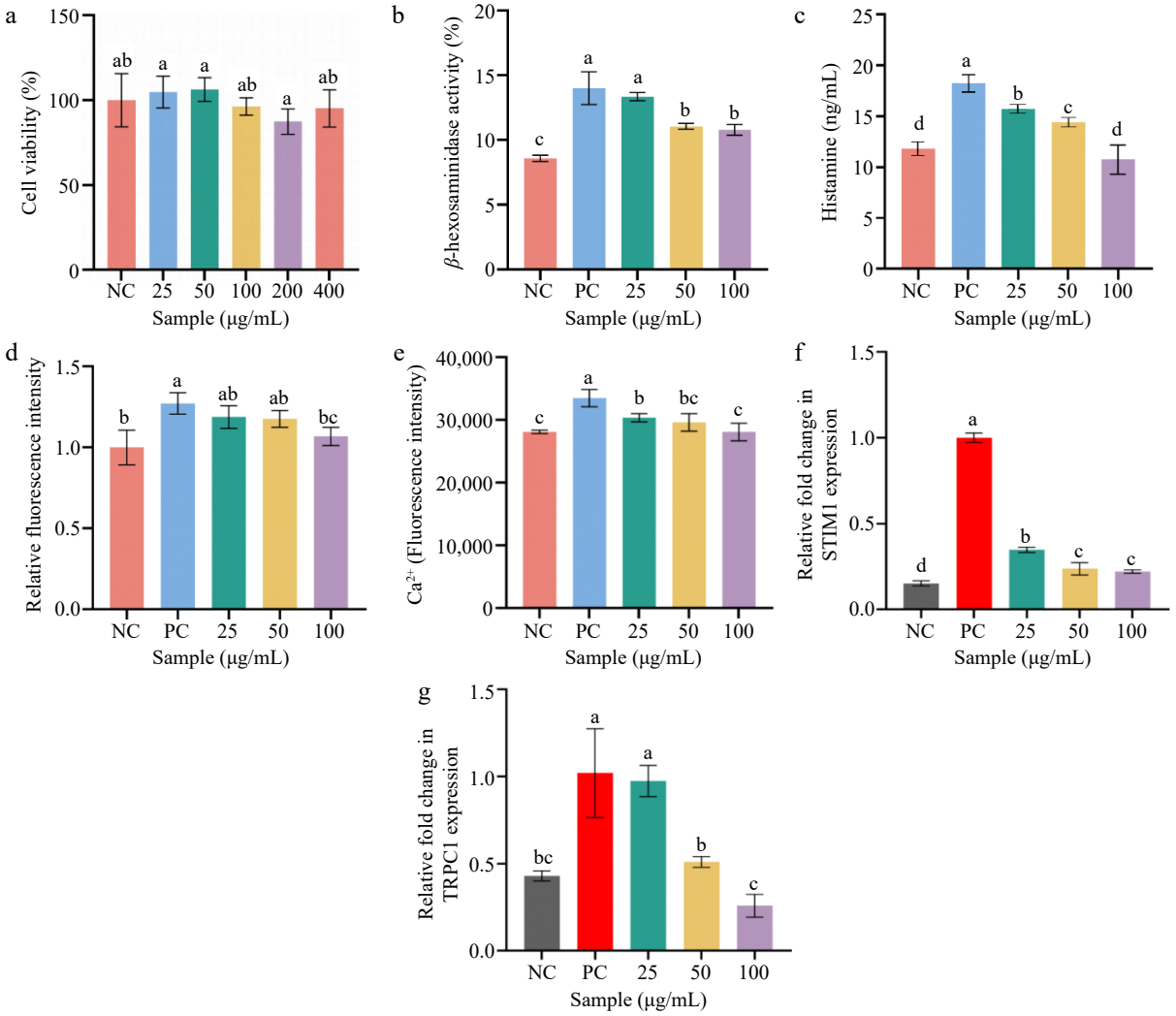

Fig. 6 The anti-allergic effects of LJF-2. (a) Cell viability of RBL-2H3 mast cells treated with LJF-2. (b) Effects of LJF-2 on β-hexosaminidase activity. (c) Effects of LJF-2 on histamine secretion. (d) Effects of LJF-2 on ROS secretion. (e) Effects of LJF-2 on Ca^{2+} secretion. (f) Effects of LJF-2 on STM1 expression. (g) Effects of LJF-2 on TRPC1 expression. Note: LJF: *Laminaria japonica* fucoidan; LJF-1: *Laminaria japonica* fucoidan with 0.5 mol/L NaCl elution; LJF-2: *Laminaria japonica* fucoidan with 1.0 mol/L NaCl elution; NC: Negative Control (untreated cells); Positive Control (LPS-stimulated cells).

levels of STIM1 and TRPC1 were investigated in this work. As shown in Fig. 6f, g, the C48/80 stimulation upregulated the expression of STIM1 and TRPC1 genes, while LJF-2 intervention (25, 50, and 100 μg/mL) significantly downregulated the gene expression of STIM1 (to 0.34, 0.23, and 0.22, respectively), and TRPC1 (to 0.97, 0.51, and 0.26, respectively) in a dose-dependent manner. These results indicated that LJF-2 treatment significantly inhibited the extracellular calcium influx by downregulating the expression of calcium channel proteins (STIM1 and TRPC1) in RBL-2H3 mast cells, thereby reducing cellular degranulation and histamine release.

Discussion

The anti-allergic activity of fucoidans is fundamentally governed by their structural properties, particularly monosaccharide composition and sulfate content[39–42]. The 1.0 mol/L NaCl-eluted fraction LJF-2 demonstrated superior anti-allergic efficacy, attributed to its high sulfate (35.07%), and uronic acid (17.20%) content, which facilitate receptor recognition and immunomodulation[20]. Structural analysis revealed prominent hydroxyl absorption (3,433 cm^{-1}), and low esterification, enhancing reactivity[43]. Enriched in rhamnose (21.42%), LJF-2 suppressed oxidative/nitrosative stress and pro-inflammatory cytokines (IL-1β, IL-6, TNF-α) in LPS-stimulated RAW264.7 cells. Its colloidal stability, evidenced by a particle size of 910.2 ± 21.8 nm and high zeta potential, promoted receptor engagement and rapid bioactivity[44–46]. These findings establish a clear structure–function relationship for LJF-2's anti-allergic action.

Moreover, the structural characterization confirmed LJF-2 possesses elevated sulfate (35.07%), and uronic acid (17.20%) content, alongside a high rhamnose composition (21.42%), which are critical for bioactivity[33]. Its superior colloidal stability (zeta potential: −44.83 mV) ensures sustained bioavailability and enhances hyaluronidase inhibition[11,46]. In RAW264.7 macrophages, LJF-2 dose-dependently suppressed LPS-induced ROS/NO production and pro-inflammatory cytokines (IL-1β, IL-6, TNF-α), disrupting inflammatory amplification[2,3,47]. In RBL-2H3 mast cells, it inhibited β-hexosaminidase and histamine release by modulating Ca^{2+} influx via the STIM1/TRPC1 pathway, concurrently reducing ROS generation[3,38,48]. The dual modulation of mast cell degranulation and macrophage activation positions LJF-2 as a promising multi-target anti-allergic agent[49].

In summary, LJF is a structurally complex macromolecule with multiple bioactivities. In this study, fractions obtained via stepwise

NaCl elution were analyzed for composition and anti-allergic potential. Variations in NaCl concentration significantly affected chemical profiles and biological activity. Specifically, elution with 1.0 mol/L NaCl yielded a fraction (LJF-2) enriched in uronic acid and sulfate groups, accompanied by reduced protein content. Structural analysis by monosaccharide composition and FT-IR confirmed heterogeneous polyanionic features. LJF-2 showed the strongest inhibition of hyaluronidase and, in cellular models, suppressed NO, ROS, and pro-inflammatory cytokine expression (IL-1β, IL-6, TNF-α) in LPS-stimulated macrophages, while also inhibiting degranulation and histamine release in activated mast cells. These results indicate that *Laminaria japonica* fucoidan, particularly the 1.0 mol/L NaCl-eluted fraction, exhibits promising anti-allergic properties, though further in vivo and clinical studies are needed to confirm its therapeutic applicability.

Conclusions

This study systematically investigated the anti-allergic properties of *Laminaria japonica* fucoidan fractions fractionated via NaCl gradient elution. Compositional analysis revealed that the fraction eluted with 1.0 mol/L NaCl (LJF-2) was enriched in sulfate groups and uronic acids, correlating with its superior hyaluronidase inhibition. Structural characterization by FT-IR confirmed key functional groups contributing to its polyanionic nature. In cellular models, LJF-2 demonstrated potent dose-dependent suppression of allergic mediators: it inhibited NO/ROS production and downregulated IL-1β, IL-6, and TNF-α expression in LPS-stimulated RAW264.7 macrophages, while also reducing degranulation and histamine release in activated RBL-2H3 mast cells. These results highlight LJF-2 as a promising natural anti-allergic agent, warranting further *in vivo* validation and mechanistic exploration for potential therapeutic applications.

Authors contributions

The authors confirm their contributions to the paper as follows: data curation: Wu X, Wang W, She Y, Yang J, Huang X, Li Z; investigation, formal analysis, writing—original draft: Wu X, Wang W, She Y, Yang J, Huang X, Li Z, Zhang Z; writing—review and editing: Li Z, Lin H, Xiao H, Zhang Z; visualization, supervision, funding acquisition, validation, project administration, conceptualization: Zhang Z. All authors reviewed the results and approved the final version of the manuscript.

Data availability

All data generated or analyzed during this study are included in this published article and its supplementary information files. Additional data are available from the corresponding author upon reasonable request.

Acknowledgements

The work was financially supported by National Natural Science Foundation of China (32572710). The authors acknowledge the assistance of Analysis and Testing Center, College of Food Science and Engineering, Ocean University of China.

Conflict of interest

The authors declare that they have no conflict of interest.

Dates

Received 12 December 2025; Revised 17 January 2026; Accepted 19 January 2026; Published online 9 March 2026

References

[1] Zhang Z, Zhao Y, Han Y, Yang B, Lin H, et al. 2022. The natural substances with anti-allergic properties in food allergy. *Trends in Food Science & Technology* 128:53–67

[2] Anjana K, Arunkumar K. 2024. Brown algae biomass for fucoxanthin, fucoidan and alginate; update review on structure, biosynthesis, biological activities and extraction valorisation. *International Journal of Biological Macromolecules* 280:135632

[3] Li HY, Yi YL, Guo S, Zhang F, Yan H, et al. 2022. Isolation, structural characterization and bioactivities of polysaccharides from *Laminaria japonica*: a review. *Food Chemistry* 370:131010

[4] Moreira ASP, Gaspar D, Ferreira SS, Correia A, Vilanova M, et al. 2023. Water-soluble *Saccharina latissima* polysaccharides and relation of their structural characteristics with *in vitro* immunostimulatory and hypocholesterolemic activities. *Marine Drugs* 21:183

[5] Bisso BN, Jahan H, Dzoyem JP, Choudhary MI. 2025. Quinic acid enhances kanamycin efficacy against methicillin-resistant *Staphylococcus aureus* biofilms. *Microbial Pathogenesis* 198:107145

[6] Álvarez-Viñas M, Torres MD, Domínguez H. 2025. Microwave-assisted depolymerization of hydrothermally extracted carrageenan from *Chondrus crispus*. *Algal Research* 89:104046

[7] Roy D, Sobuj MKA, Islam MS, Haque MM, Islam MA, et al. 2024. Compositional, structural, and functional characterization of fucoidan extracted from *Sargassum polycystum* collected from Saint Martin's Island, Bangladesh. *Algal Research* 80:103542

[8] Li Z, Zhang Z, Feng Y, Guo Y, Li Z, et al. 2025. Insight into the anti-inflammatory sulfated polysaccharides from *Sargassum carpophyllum* and structure-function relationships. *Algal Research* 85:103841

[9] Shi H, Wan Y, Li O, Zhang X, Xie M, et al. 2020. Two-step hydrolysis method for monosaccharide composition analysis of natural polysaccharides rich in uronic acids. *Food Hydrocolloids* 101:105524

[10] AlBathish M, Gazy A, Al Jamal M, Bejjani A. 2024. Utilization of the FTIR spectroscopic method for the quantitative determination of the narrow therapeutic index levothyroxine sodium in pharmaceutical tablets. *Pharmacia* 71:1–9

[11] Xiong W, Li J, Li B, Wang L. 2019. Physicochemical properties and interfacial dilatational rheological behavior at air-water interface of high intensity ultrasound modified ovalbumin: effect of ionic strength. *Food Hydrocolloids* 97:105210

[12] Lei W, Liu C, Pan L, Peng C, Wang J, et al. 2021. Screening of probiotic *Lactobacilli* with potential anti-allergic activity based on hyaluronidase inhibition and degranulation of RBL-2H3 cells *in vitro*. *LWT* 140:110707

[13] Wagner A, Alam SB, Kulka M. 2023. The effects of age, origin, and biological sex on rodent mast cell (BMMC and MC/9) and basophil (RBL-2H3) phenotype and function. *Cellular Immunology* 391:104751

[14] Lin XT, Zhang J, Xie CM. 2023. An optimized protocol to detect protein ubiquitination and activation by ubiquitination assay *in vivo* and CCK-8 assay. *STAR Protocols* 4:102199

[15] Ishida M, Matsubara I, Yamauchi S, Nishi K, Sugahara T. 2025. Correlation between the biological activities and the chemical structures of conidendrin-related compounds: (–)-β-conidendrin inhibits degranulation of RBL-2H3 cells. *Bioscience, Biotechnology, and Biochemistry* 89:795–804

[16] Passante E, Ehrhardt C, Sheridan H, Frankish N. 2009. RBL-2H3 cells are an imprecise model for mast cell mediator release. *Inflammation Research* 58:611–618

[17] Lakshmana Senthil S. 2024. A comprehensive review to assess the potential, health benefits and complications of fucoidan for developing as functional ingredient and nutraceutical. *International Journal of Biological Macromolecules* 277:134226

[18] Zhong R, Wan X, Wang D, Zhao C, Liu D, et al. 2020. Polysaccharides from marine *Enteromorpha*: structure and function. *Trends in Food Science & Technology* 99:11–20

[19] Chen BJ, Qiao YJ, Yu G, Wang X, Zhang Y, et al. 2024. Sulfation, characterization, antibacterial activity, and action mechanism of rice bran polysaccharides. *Food Bioscience* 59:103953

[20] Cui Z, Wang H, Qin L, Yuan Y, Xue J, et al. 2025. Probing the structural elements of polysaccharide adjuvants for enhancing respiratory mucosal response: from surmounting multi-obstacles to eliciting cascade immunity. *ACS Nano* 19:11012−11028

[21] Mulloy B. 2005. The specificity of interactions between proteins and sulfated polysaccharides. *Anais da Academia Brasileira de Ciencias* 77:651−664

[22] Heo JH, Je JG, Sim JH, Ryu B, Heo SJ, et al. 2024. Quantitative analysis of fucose in fucoidans from *Sargassum* spp. in Jeju Island, South Korea using 3-methyl-1-phenyl-5-pyrazolone derivatization and RP-HPLC-UV method. *Algal Research* 79:103441

[23] Nagahawatta DP, Liyanage NM, Jayawardena TU, Yang F, Jayawardena HHACK, et al. 2023. Functions and values of sulfated polysaccharides from seaweed. *Algae* 38:217−240

[24] Lee HG, Jayawardhana HHACK, Yang F, Nagahawaththa DP, Liyanage NM, et al. 2024. Anti-obesity effects of fucoidan from *Sargassum thunbergii* in adipocytes and high fat diet induced obese mice through inhibiting adipogenic specific transcription factor. *Food Science and Human Wellness* 13:1608−1616

[25] Liao Q, Pang L, Li JJ, Zhang C, Li JX, et al. 2022. Characterization and diabetic wound healing benefits of protein-polysaccharide complexes isolated from an animal ethno-medicine *Periplaneta americana* L. *International Journal of Biological Macromolecules* 195:466−474

[26] Shu Y, Li J, Yang X, Dong X, Wang X. 2019. Effect of particle size on the bioaccessibility of polyphenols and polysaccharides in green tea powder and its antioxidant activity after simulated human digestion. *Journal of Food Science and Technology* 56:1127−1133

[27] Wang S, Yang J, Shao G, Qu D, Zhao H, et al. 2020. Soy protein isolated-soy hull polysaccharides stabilized O/W emulsion: effect of polysaccharides concentration on the storage stability and interfacial rheological properties. *Food Hydrocolloids* 101:105490

[28] Zhang K, Chen C, Huang Q, Li C, Fu X. 2022. Preparation and characterization of *Sargassum pallidum* polysaccharide nanoparticles with enhanced antioxidant activity and adsorption capacity. *International Journal of Biological Macromolecules* 208:196−207

[29] Nawy SS, Csóka AB, Mio K, Stern R. 2001. Hyaluronidase activity and hyaluronidase inhibitors: assay using a microtiter-based system. In *Proteoglycan Protocols*, ed. Iozzo RV. Totowa, NJ: Humana Press. pp. 383−389 doi: 10.1385/1-59259-209-0:383

[30] Nagaraju S, Girish KS, Pan Y, Easely KA, Kemparaju K. 2011. Estimation of serum hyaluronidase activity overcoming the turbidity interference. *American Society for Clinical Laboratory Science* 24:172−177

[31] Li C, Sun H, Gu X, Long W, Zhu G, et al. 2025. Exploring the inhibitory effects of fucosylated chondroitin sulfate (FCS) oligosaccharide isolated from *Stichopus horrens* and the derivatives on P-selectin. *Marine Drugs* 23:236

[32] Schmaus A, Spataro S, Sallmann P, Möller S, Scapozza L, et al. 2025. A novel, cell-compatible hyaluronidase activity assay identifies dextran sulfates and other sulfated polymeric hydrocarbons as potent inhibitors for CEMIP. *Cells* 14:101

[33] Li C, Tian Y, Pei J, Zhang Y, Hao D, et al. 2023. Sea cucumber chondroitin sulfate polysaccharides attenuate OVA-induced food allergy in BALB/c mice associated with gut microbiota metabolism and Treg cell differentiation. *Food & Function* 14:7375−7386

[34] Yang Z, Wali A, Arken A, Dongmulati N, Hu A, et al. 2024. Purification and characterisation of a homogenised protein from Red Deer (*Cervus elaphus*) abomasum as a potential hyaluronidase inhibitor. *International Journal of Food Science and Technology* 59:9108−9116

[35] Jayasinghe AMK, Kirindage KGIS, Fernando IPS, Kim KN, Oh JY, et al. 2023. The anti-inflammatory effect of low molecular weight fucoidan from *Sargassum siliquastrum* in lipopolysaccharide-stimulated RAW 264.7 macrophages via inhibiting NF-κB/MAPK signaling pathways. *Marine Drugs* 21:347

[36] Zhang J, Hong L, Zhang P, Wang Y, Hong T. 2023. Inhibitory effect of daphnetin on the C48/80-induced pseudo-allergic reaction. *International Immunopharmacology* 124:110874

[37] Zhang W, Tang R, Ba G, Li M, Lin H. 2020. Anti-allergic and anti-inflammatory effects of resveratrol via inhibiting TXNIP-oxidative stress pathway in a mouse model of allergic rhinitis. *World Allergy Organization Journal* 13:100473

[38] Lim S, Oh S, Nguyen QTN, Kim M, Zheng S, et al. 2023. *Rosa davurica* inhibited allergic mediators by regulating calcium and histamine signaling pathways. *Plants* 12:1572

[39] Qiu Z, Qiao Y, Zhang B, Sun-Waterhouse D, Zheng Z. 2022. Bioactive polysaccharides and oligosaccharides from garlic (*Allium sativum* L.): production, physicochemical and biological properties, and structure-function relationships. *Comprehensive Reviews in Food Science and Food Safety* 21:3033−3095

[40] Jiang Y, Zhao Y, Liu Z, Fang JK, Lai KP, et al. 2024. Roles and mechanisms of fucoidan against dermatitis: a review. *International Journal of Biological Macromolecules* 279:135268

[41] Kim AR, Kim MJ, Seo J, Moon KM, Lee B. 2024. The beneficial roles of seaweed in atopic dermatitis. *Marine Drugs* 22:566

[42] Jia N, Zhang S, Chen R, He X, Dai C, et al. 2025. Immunomodulatory functions of algal bioactive compounds. *Critical Reviews in Food Science and Nutrition* 65:7133−7150

[43] Yuan L, Qiu Z, Yang Y, Liu C, Zhang R. 2022. Preparation, structural characterization and antioxidant activity of water-soluble polysaccharides and purified fractions from blackened jujube by an activity-oriented approach. *Food Chemistry* 385:132637

[44] Li D, Wei R, Zhang X, Gong S, Wan M, et al. 2024. Gut commensal metabolite rhamnose promotes macrophages phagocytosis by activating SLC12A4 and protects against sepsis in mice. *Acta Pharmaceutica Sinica B* 14:3068−3085

[45] Alhussain H, Alghamdi AM, Elamin NY, Rajeh A. 2024. Recent progress in enhanced optical, mechanical, thermal properties, and antibacterial activity of the chitosan/polyvinylalcohol/Co_3O_4 nanocomposites for optoelectronics and biological applications. *Journal of Polymers and the Environment* 32:3735−3748

[46] Németh Z, Csóka I, Semnani Jazani R, Sipos B, Haspel H, et al. 2022. Quality by design-driven zeta potential optimisation study of liposomes with charge imparting membrane additives. *Pharmaceutics* 14:1798

[47] Kwon DH, Cha HJ, Choi EO, Leem SH, Kim GY, et al. 2018. Schisandrin A suppresses lipopolysaccharide-induced inflammation and oxidative stress in RAW 264.7 macrophages by suppressing the NF-κB, MAPKs and PI3K/Akt pathways and activating Nrf2/HO-1 signaling. *International Journal of Molecular Medicine* 41:264−274

[48] Nagata Y, Suzuki R. 2022. FcεRI: a master regulator of mast cell functions. *Cells* 11:622

[49] Higashio H, Yokoyama T, Saino T. 2024. A convenient fluorimetry-based degranulation assay using RBL-2H3 cells. *Bioscience, Biotechnology, and Biochemistry* 88:181−188